
Article:
Arsenyeva, A., Duddeck, F. and Thompson, H.M. (2024) An iso-contour method for automated fiber placement optimization of composite structures. Composite Structures, 327. 117628. ISSN: 0263-8223

https://doi.org/10.1016/j.compstruct.2023.117628

An iso-contour method for automated fiber placement optimization of composite structures

Anna Arsenyeva*[1], Fabian Duddeck†[1] and Harvey M. Thompson‡[2]

[1]Department of Civil, Geo, and Environmental Engineering, Technical University of Munich
[2]School of Mechanical Engineering, University of Leeds

October 22, 2023

Abstract

A new method for numerical optimization of fiber-steered composites is presented, which allows to control efficiently and effectively the curvature of the fibers of single- or multi-layer composite structures. It is based on the introduction of an artifical surface defined and controlled by a relatively small number of control points, which is optimized to identify optimal fiber orientations varying smoothly over the panels. Curvature constraints like the maximum fiber curvature constraint, MFCC, or the average fiber curvature constraint, AFCC, are respected explicitly by the method to ensure manufacturability of the composite component. Three validation cases are regarded where results of the unconstrained case are compared to those of established methods to illustrate the validity of the new approach. They are complemented by results considering curvature constraints showing that optimal structures depend strongly on the chosen curvature thresholds. Finally, a rib optimization of a wingbox structure is realized as a more complex case.

1 Introduction

Composite materials based on carbon or glass fiber reinforced polymers (CFRP, GFRP) are widely used for aerospace or other structures. One of the main advantages here is the possibility to tailor the material according to dominant load directions, which is normally done by selecting and/or optimizing the stacking sequence and the orientations of a set of unidirectional layers. This can be improved by adapting the composite layout more locally to the directions of the stress field employing an automated fiber placement (AFP) technology [1]; the outcome is also known as fiber-steered composites (FSC) [2, 3], or variable stiffness (VS) fiber-placed composite laminates [4, 5, 6, 7, 8, 9]. Fibers are placed

*anna.arsenyeva@tum.de
†duddeck@tum.de
‡H.M.Thompson@leeds.ac.uk

along curvilinear paths within the plane of the laminate, tailoring mechanical properties like stiffness, buckling resistance, aero-elastic and/or vibrational properties.

When designing and optimizing fiber-steered composites, the manufacturing procedure has to be considered with its inherent requirements. Normally, a robot arm places one or more uni-directional fiber tows following a predefined path on an arbitrary surface. This may result in manufacturing problems, such as local tow gaps, steering overlaps, tow pull-up/tow misalignment, wrinkling/buckling, or even fiber failure [8]. To avoid this, a minimum turning radius or maximum curvature of the fiber tow paths has to be respected [1]. Related factors such as pressure of the AFP roller, heating source/process temperature, or material tackiness may lead to additional restrictions. Nevertheless, main constraints for numerical optimization are given by thresholds for fiber in-plane curvature and material width. The former is normally defined by restricting the minimum radius for the centerline of the fiber-course [1], while the latter can be addressed directly as band width of the tow.

The numerical optimization of structures with standard CFRP/GFRP materials is already of high complexity requiring special methods [10]. Beside shape and topology parameters defining the global geometry, design variables related to stacking sequence, layer thicknesses, and fiber orientations are of interest. This leads to optimization problems with a mixture of continuous and discrete variables. The corresponding objectives and/or constraints, e.g. compliance or buckling resistance, are therefore often non-convex and multi-modal; i.e. there is not a unique solution. This situation becomes even more challenging in case of VS/FSC where additional design parameters are introduced describing local lay-ups and orientations at every point of the structure. Fiber continuity and laminate manufacturability have to be ensured, which leads not only to problems with a very high number of design parameters but also with a large number of local constraints. For parametrization, different approaches have been discussed in the literature; the corresponding state of the art is summarized in the next section.

2 State of the Art

Approaches using directly FE elements or patches: Direct variation of fiber paths represents the first group of methods for designing and optimizing fiber-steered composite materials. The proposed techniques control either fiber orientation for each FE element or they use larger patches of elements with constant laminate properties to reduce the number of design parameters [11, 12]. Providing less freedom for spatial variation of fiber direction, patches allow easier consideration of manufacturing requirements. However, the obtained optimal design is strongly pre-determined by the chosen patch geometry or patch material properties. The other approach is based on an iterative derivation of principal stress directions to identify fiber angles. Here, the fiber angles are not varied during the optimization but are defined as a result of the FE simulation such that the material data has to be updated and the simulations are repeated [13]. Another example where fiber orientations are directly taken as design variables is presented by Setoodeh [14, 15]. Here, the domain is divided into a large number of rectangular cells, and a cellular automaton (CA) is ap-

plied with special update rules for field and design variables to iteratively find the optimal design. Additional heuristic pattern-matching rules are applied in order to improve manufacturability of the obtained designs.

Parametric path approaches: To reduce the number of design variables, a one-dimensional parametric description of fiber paths can be chosen. The changing paths are then defined on the geometry level and do not require design domain discretization using elements or patches of elements, see for example the work of Gürdal et al. [16, 17] and later Alhajahmad et al. [18] and Stanford et al. [19]. The fiber path orientations, for example, can be changed linearly from one end of the panel to the other along one axis. This parametrization allows to explicitly derive the fiber paths and obtain curvature radius to consider manufacturability [18]. Results indicate that even with simple linear variation of fiber orientation, significant design improvements can be achieved compared to classical uni-directional laminates. Alhajahmad et al. [2] also investigated nonlinear angle variation based on Lobatto-–Legendre polynomials. Alternatively, Nagendra et al. [33] proposed to represent fiber paths as a weighted sum of predefined one-dimensional basis fiber curves (non-uniform rational basis splines, NURBS) and to vary the weights to achieve improved or optimized fiber layouts.

Huang and Haftka [20] proposed optimization of fiber orientations based on a 2D fiber path parametrization. To optimize a structure around a hole, fiber angles in the vicinity of the hole are represented using piecewise bilinear interpolation functions. Brooks et al. [21] used tensor products of B-splines to define fiber angle variations over the design domain. The authors mention several desired properties of such parametrization, including flexibility due to arbitrary number of control points, smoothness of the resulting fiber paths and compact support of splines, making a change of a single control point to have only local effect. Smoothness of the fiber paths was controlled by increasing or decreasing the number of control points, which provides an option to include curvature constraints within the optimization. It was also shown, that for relatively simple plate-in-bending problems, a gradient-based optimizer can be trapped in a local optimum, which motivates the use of global optimization methods.

Another approach was presented by Honda et al. [22] where the fiber path distribution is defined by contour lines of cubic polynomials specified over a 2D plate domain. Polynomial coefficients are manipulated directly in order to vary fiber paths. This approach can be viewed as an implicit parametrization, as no explicit path parametrization is defined. The method uses the average curvature condition for manufacturability of fiber curvature, see also [23]. A multi-objective optimization was realized showing that average curvature as first objective is clearly conflicting with structural criteria like first eigenfrequency or Tsai-Wu failure index as second objective.

LP-based approaches: To reduce complexity, the optimization can be divided into two steps, see some of the early approaches for standard composites [24, 25]. Here, the first optimization stage consists in optimizing the so-called lamination parameters (LPs) and the second identifies the stacking sequence which fulfils the optimal values of the lamination parameters. The 12 lamination parameters where introduced by Tsai et al. [26, 27] and represent together with material invariants the stiffness tensors of laminated composites

based on a set of uni-directional laminae; they are trigonometric functions of the ply orientations. Because the LPs are interrelated, additional inequality constraints have to be introduced to describe the feasible regions for the LPs. These regions are convex as shown in [28]. Both, the reduction of the number of design variables by using LPs and the convexity of the design space are advantageous for numerical optimizations.

For the second step, the identification of the lay-up fulfilling the optimized LPs, new methods are required to enable optimization of AFP design problems. Here, after identifying the optimal distribution of LPs, the corresponding stacking sequences and fiber paths have to be determined. This is not a trivial task and, in fact, is another optimization problem with no closed-form solution. Moreover, assuming a predefined number of layers, no laminate lay-up exists for some points in the LP space. In this case, a least squares problem can be used to find the best possible stacking for the optimal LPs, as proposed by van Campen et al. [29]. Because of non-convexity of this problem, a genetic algorithm was used by the authors together with a cellular automata method. Once the layer-wise optimal stacking sequence is obtained, the discrete element-wise values of fiber angles within each layer need to be converted into continuous paths; further details are given in [30, 5]. For single-layer problems, Setoodeh et al. [31] proposed to identify fiber paths corresponding to optimal LP distributions using also a least-squares formulation where the paths were parametrized via Lobatto polynomials. Klees et al. [32] used hierarchical shape functions to parametrize fiber angles for multi-layered composite rectangular plates, which were optimized for maximum buckling load using LPs. The studies showed that shape functions of higher order are more efficient than increasing the number of laminate layers. Blom et al. [3] developed an approach converting the given fiber orientations into continuous fiber paths using a streamline-analogy. How to integrate here the local conditions on fiber curvature is, to the knowledge of the authors, an open question.

To conclude the state of the art section, it can be noted that there is a number of parametrization approaches for AFP composites but they differ strongly concerning their complexity (number of parameters) and their ability to account for manufacturability (maximum curvature control). The main target of the current work was to develop a new method which would allow to describe big variety of fiber paths without a high parameter or constraint dimensionality, at the same time providing an efficient way to integrate curvature constraints, which resulted into the Iso-Contour Method (see Section 4). Before this is presented in detail, different ways to consider manufacturing requirements are discussed in the next section.

3 Manufacturing requirements

As described in the introduction, it is necessary to control the fiber curvature; high curvatures lead to various imperfections of the material and/or violate capabilities of existing AFP machines. Thus, manufacturability of the obtained fiber layout should be addressed during the optimization. In literature, there are different ways to realize this; most of them use either the average fiber curvature constraint (AFCC) or the maximum fiber curvature constraint (MFCC). In cases, where a parametric description of fiber paths is used, the curvature can

be directly derived from the one-dimensional parametric curves [2, 18, 17, 33, 19] or the two-dimensional representations, e.g. [21, 22]. Then, the obtained curvature can be averaged over the design space for AFCC (e.g. [22]) or directly used to obtain the curvature maximum for MFCC. The same techniques can also be applied when converting LP-based optimization results into fiber paths using least-squares formulations with explicit path parametrizations [32, 31]. Often, discrete (element-wise) parametrization of fiber angles is used, such that linear shape functions can be defined over the elements to approximate the angle variation. Then, the curvature is calculated as the rate of change in fiber angles, see e.g. [30, 23] to determine the MFCC. For the AFCC, the element-wise curvature information can be assembled into a layer representation of the curvatures to compute the average fiber curvature as proposed for example in [34, 23]. A similar approach can be used in case the streamline analogy is used to limit the streamlines' curvatures [3]. Note that in general, the AFCC approach cannot guarantee that designs are manufacturable w.r.t. maximum curvature; but they can provide an improvement over an unconstrained design while being less complicated for an optimizer than the maximum curvature constraint. In contrast, the MFCC captures accurately local curvature conditions but leads to a high number of values to be considered in the optimizations, which increases complexity therefore is not optimal. Hence, a new approach is proposed in the next section using an iso-contour approach.

4 Iso-contour method

In this section, the main steps of the proposed 2D fiber steering optimization method, the 'Iso-Contour Method' (ICM), are described. The main idea without details was introduced in [35, 36, 34]; further aspects including an embedding into an overall hierarchical optimization of aerospace structures are given in [37]. The key idea of the proposed method is to use an artificial parametric surface defined over the 2D structural domain to control fiber paths. In a certain way, this can be understood like a level-set function; although, we do not consider only the zero-level boundary, but the gradients of the surface describing the fiber orientations and their changes. The smoothness of this surface controls the continuity and smoothness of the fiber steering.

The scheme of the method is presented in Fig. 1. To introduce the artificial contour function, a 2D box domain is created in a first step containing completely the structural component. Then, a grid of control points (could also be non-regular) is defined inside this box. This may be identical or non-identical to the finite element (FE) nodes. The number and the locations of these control points are user-defined. To each control point an initial height value is assigned, which is then varied within the optimization. The artificial surface is finally created using standard regression or interpolation algorithms from meta-modeling approaches, e.g. described in [38]. In the current work, non-parametric surfaces are used, such as Radial Basis Functions (RBF), Gaussian Process Interpolation (GP), or 2D splines. Splines interpolation requires regular grid positioning of the control points, while RBF and GP allow flexible point locations. The locations of the control points can be adjusted to fit specific geometrical elements (e.g. holes) allowing more flexibility for fiber paths where necessary. As for geodesic

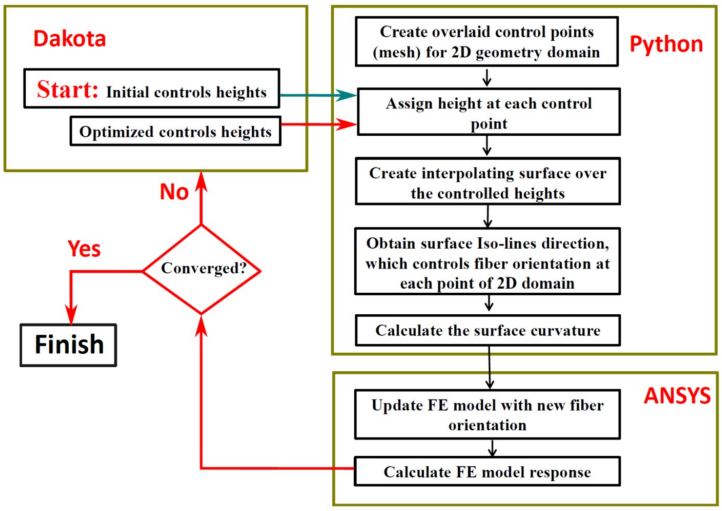

Figure 1: Workflow of the proposed Iso-Contour Method.

maps, the iso-contour lines are obtained from this artificial surface. These iso-contours guide the fiber paths at each point of the 2D structural domain, with the fiber directions aligned locally to the iso-contour lines. The curvature can be also obtained from these isolines.

For the optimization, the 'heights' defined at the control points are considered as design variables, which means that the number of control points represents the dimension of the optimization problem. The results presented here are meant to illustrate the Iso-Contour Method. Hence, the focus is put on identifying optimal fiber orientations; other parameters (e.g. related to the stacking sequence) of composite materials are not considered in the optimizations. It is therefore assumed that the homogenized properties of the fiber reinforced composite are already known; they are inserted into the orthotropic material model of the FE code. In this case, the main principal axis of this orthotropic material is aligned with the fiber direction. Changing of the fiber direction of the composite is then equal to rotating the material's principal axes. As a consequence, the method can be easily used together with commercial 'black box' FE codes, especially if non-intrusive implementations are required. Via rotation of the local coordinate systems (LCS) for each element, the fiber alignment according to the iso-contour lines passing through the element centroid can be realized.

Curvature handling: As discussed in Section 3, maximum curvature of fiber paths must be limited to assure manufacturable fiber-steered composite designs. This paragraph shows how this constraint is included within the proposed method for mono- or multi-layered designs. The distribution of the fiber angles in the design domain can be viewed as a vector field $\mathbf{V}$, defined by

$$\mathbf{V} = u(x,y)\mathbf{e}_x + v(x,y)\mathbf{e}_y, \tag{1}$$

where u and v are the x, y components of the fiber directions. $\mathbf{e}_x, \mathbf{e}_y$ are the Cartesian unit vectors. With this definition, the absolute curvature of the vector

field $\mathbf{V}$ can be expressed by (see e.g. [39]):

$$k_{x,y} = \left| \frac{u^2 v_x - v^2 u_y + uv(v_y - u_x)}{(u^2 + v^2)^{3/2}} \right|, \tag{2}$$

where subscripts x, y denote partial derivatives w.r.t x and y, respectively. The fiber directions are derived from the artificial surface $\varphi(x, y)$ as tangents to the iso-contours, i.e.:

$$u = \frac{\partial \varphi}{\partial y} = \varphi_y; \qquad v = -\frac{\partial \varphi}{\partial x} = -\varphi_x; \tag{3}$$

choosing a special value $\varphi(x, y) = C$ as particular contour line. Using Eqs. (1,2) leads to

$$k_c = \left| \frac{\varphi_{xx}\varphi_y^2 - 2\varphi_{xy}\varphi_x\varphi_y + \varphi_{yy}\varphi_x^2}{(\varphi_x^2 + \varphi_y^2)^{3/2}} \right|. \tag{4}$$

For the important case of multi-layered composite materials, layers are designed interdependently, e.g. using reflected or rotated layers w.r.t. the baseline layer. In the case of reflection, the fiber angle α is changed to $-\alpha$ for each point of the geometry domain. This can be expressed mathematically as:

$$u^{[-\alpha]} = u = \frac{\partial \varphi}{\partial y}; \qquad v^{[-\alpha]} = -v = \frac{\partial \varphi}{\partial x}. \tag{5}$$

Inserting these expressions into (2) leads to

$$k_c^{[-\alpha]} = \left| \frac{\varphi_{xx}\varphi_y^2 - \varphi_{yy}\varphi_x^2}{(\varphi_x^2 + \varphi_y^2)^{3/2}} \right|. \tag{6}$$

Another option to construct new layers is to rotate fibers by $\pi/2 : \alpha \to \alpha + \pi/2$. This transformation is expressed as:

$$u^{[\pi/2]} = -v = \frac{\partial \varphi}{\partial x}; \qquad v^{[\pi/2]} = u = \frac{\partial \varphi}{\partial y}. \tag{7}$$

leading to

$$k_c^{[\pi/2]} = \left| \frac{\varphi_{xy}\left(\varphi_x^2 - \varphi_y^2\right) + \varphi_x\varphi_y(\varphi_{yy} - \varphi_{xx})}{(\varphi_x^2 + \varphi_y^2)^{3/2}} \right|. \tag{8}$$

In general, for a given rotation angle γ, the curvature can be calculated [39]:

$$k_c^{[\gamma]} = |k_c \cos\gamma + k_c^{[\pi/2]} \sin\gamma|. \tag{9}$$

Fig. 2 shows an example of fiber paths obtained from the case of a hyperbolic-paraboloid surface for a plate with hole for different layer transformations. As can be seen, the curvature for the mirrored and the rotated layer can differ significantly from the curvature of the original layer. This means that the curvature of the transformed layers needs to be considered when designing such multi-layered composites. In general, the MFCC for each layer requires to find the maximum curvature within the total geometry domain. In this work, a straightforward sampling-based approach is used here because artificial surface evaluations are very cheap. For the examples regarded here, a sampling between 200×200 and 1000×2000 grid points are used. The advantage is that the obtained MFCC values are independent from the finite element discretization.

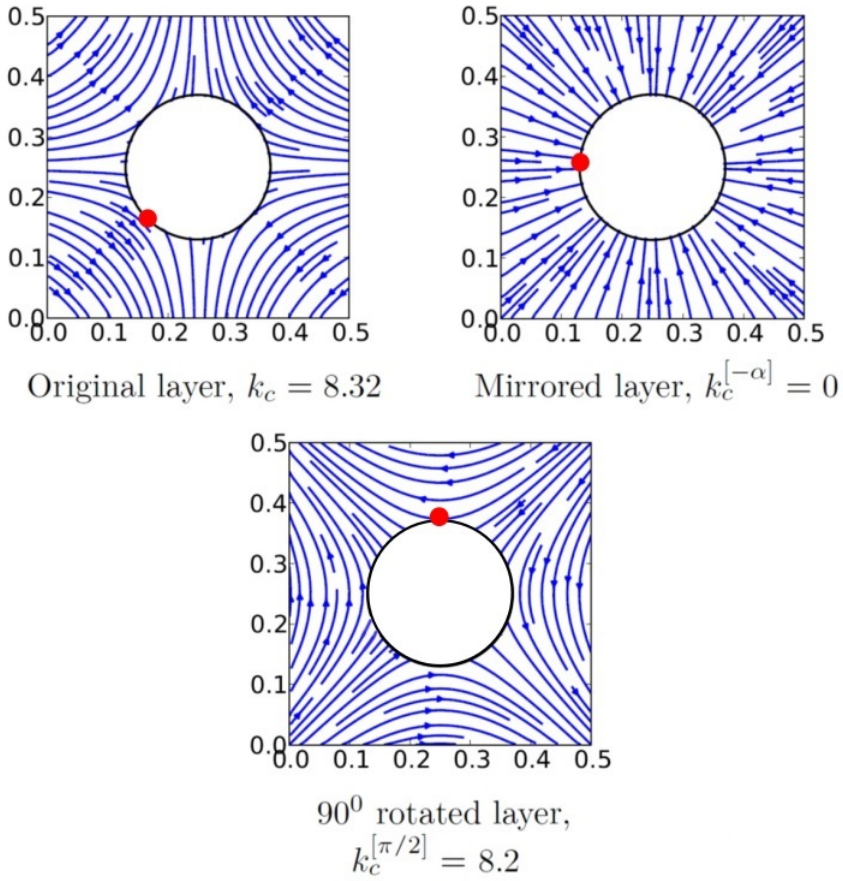

Figure 2: Example for fiber orientations for the original layer (top, left), the mirrored layer (top, right), and for the by 90° rotated layer (bottom). The numbers k_c (in m^{-1}) show the maximum curvature (MFCC) for each layer and the red dots show the corresponding locations.

Optimization approach The aim of the optimization is to find the global optimal fiber placement in order to improve desired properties of the structure (e.g. structural stiffness, maximum stress, buckling force, etc.) and at the same time to fulfil the aforementioned manufacturability constraints, formulated in terms of fiber curvature. While it is possible to compute local sensitivities of integral functions (e.g. strain energy, compliance.) w.r.t. fiber orientations within finite-elements, extreme-based quantities, such as maximum curvature or maximum equivalent stresses must be reformulated using constraint aggregation techniques (e.g Kreisselmeier-Steinhauser function), which may end up in violating original constraints. Moreover, local curvatures are highly non-linear w.r.t. design parameters, represented by the artificial surface control points, which makes the optimization problem challenging for local gradient-based methods. Thus, gradient-free global optimization methods are used within this work for handling highly non-linear curvature constraints. Flexibility of the iso-contour

parametrization allows to keep the optimization problem dimension relatively low, which makes global optimization computationally feasible. The fact, that sensitivity information is not required allows to apply the proposed technique to problems, where sensitivity information is not straightforward available (extreme problems, contact/crash applications, etc).

In particular, within this work, an evolutionary optimizer is used here for the examples on fiber-steered composite optimization. This is complemented in some cases by a local optimizer to establish a two-stage optimization, first an exploration phase via the evolutionary strategy followed by an exploitation phase using COBYLA (Constrained optimization by linear approximation). Both algorithms are provided by Dakota [40], see also [41]. The optimization algorithms are not described in detail here because the main emphasis of the work presented here lies on the parametrization and the constraint handling.

5 Validation results

To validate the proposed Iso-Contour Method, several test problems are investigated here. The first test problem consists of optimal fiber placement for a plate under two static loads; this case enables a qualitative comparison with results from classical density-based topology optimization. The second test case is inspired by the work of Setoodeh [15] where a clamped plate is optimized for maximum stiffness in bending. This problem allows direct comparison of optimal fiber placement via the proposed method and Setoodeh's work. The third test problem addresses a more complex problem; i.e. the design of a multi-layer fuselage panel for maximum buckling force where results of an LP-based optimization are available for qualitative comparison. Simulations are performed using laminate modeling capabilities of the commercial FE solver ANSYS. For all test problems, an orthotropic material represented by homogenized fiber-steered laminates are used having the following elastic properties: elastic moduli $E_1 = 130$ GPa, $E_2 = E_3 = 10$ GPa, shear moduli $G_{12} = G_{31} = 5$ GPa, $G_{23} = 27$ GPa, and Poisson's ratios $\nu_{12} = \nu_{31} = 0.35, \nu_{23} = 0.2$.

Plate under two in-plane static loads: As first test problem, a fiber path optimization for a centrally supported composite plate with two top/side loads (see Fig. 3, top left) is regarded. The dimensions of the plate are taken as 160 mm x 100 mm with a thickness of 1 mm. A single-layer laminate material is used for the plate. In total 9 points are placed in a 3×3 grid over the 2D plate domain, which control the artificial surface and define the corresponding iso-contour fiber paths. Thus, the number of design variables for this test case is equal to 9. The control points are placed on a regular grid and a bivariate spline surface is used for this example. The FE model is relatively coarse with a mesh of 16×10 shell elements (8-node 2^{nd} order shell elements). An evolutionary algorithm is employed for optimization, where the sum of the displacements of the loaded points on the top of the plate should be minimized. The first results are given here without consideration of curvature constraints.

The optimal surface reached after 100 iterations and therefore 4000 FE simulations is shown in the top row (right) of Fig. 3. The corresponding isoline results are given in the middle row (left) of the same figure. The optimal topology (obtained by Solid Isotropic Material with Penalization, SIMP) for equally

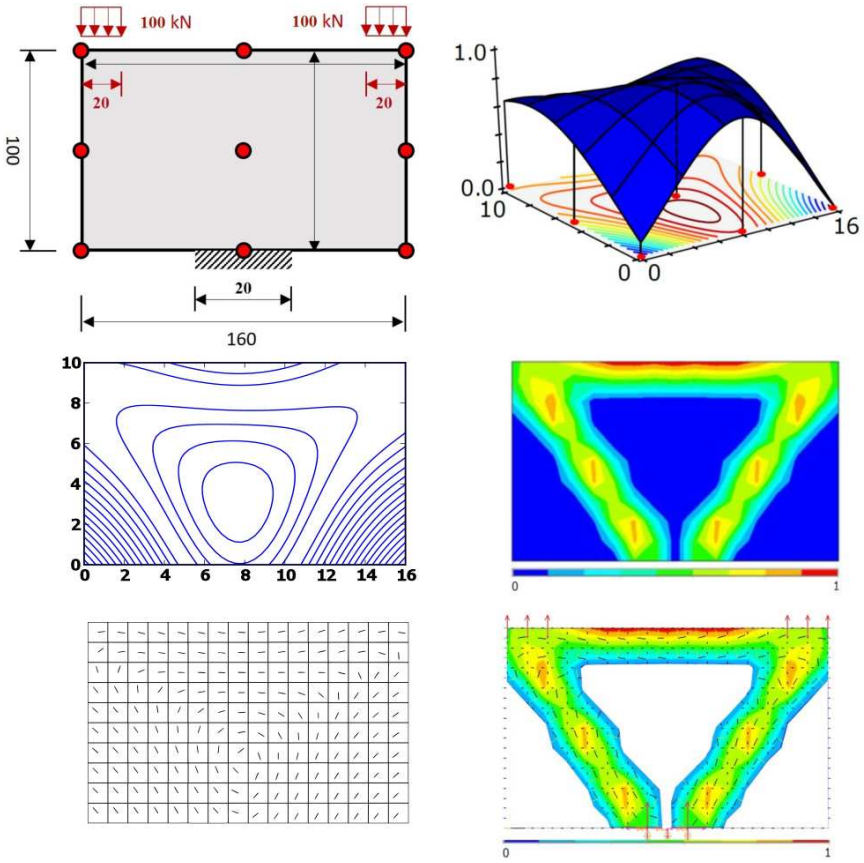

Figure 3: Results of the first test case (from left to right): Top row: Problem definition and 3D visualization of optimal contour; middle row: Optimal isolines and isotropic topology results; bottom row: Optimal fiber orientations and overlaid image of topology and fiber orientation results.

loaded isotropic design is shown in the middle row (right) of Fig. 3. In the bottom row of the same figure, the optimal fiber orientations for each FE element are shown (left without and right with the overlay of the topology result). Comparison of the results suggests, that the fiber orientations identified with the proposed iso-contour method are in this case similar to the load path directions derived from an isotropic SIMP topology optimization.

In the next step, the influence of the curvature constraints is explored. For this, several optimization runs with different curvature constraints are performed, starting with the unconstrained case from above, followed by an optimization using the average fiber curvature constraint (AFCC) with a threshold of of 0.2 m^{-1} and 0.4 m^{-1} and finally an optimization constraint by the maximum fiber curvature constraint (MFCC) with 0.2 m^{-1} and 0.4 m^{-1} as limits. The isoline results of the constraint cases are given in Fig. 4. The Table 1 summarizes the results of the optimization, listing displacement reduction factor in relationship to a displacement obtained for a simple 90° laminate solution. A

Table 1: Final values of the objective. Displacements are normalized with respect to the average displacement of a 90° laminate (constraint values in m^{-1}).

90°		AFCC	AFCC	MFCC	MFCC
-	∞	0.4	0.2	0.4	0.2
1.0	2.027	1.818	1.688	1.480	1.100

stricter (i.e. smaller) constraint value leads to design performance loss, however even the very smooth design with MFCC equal to 0.2 m^{-1} outperforms unidirectional laminate. It can be noted, that MFCC produces much smoother paths for the same constraint setting, as AFCC. The reason for that is the inability of AFCC to capture effects of high local curvatures: for example, the maximum curvature, obtained for AFCC setting 0.4 m^{-1} is 5.3 m^{-1}, and for 0.2 m^{-1} is 1.1 m^{-1}. On the other hand, AFCC is a much smoother metric of global curvature changes during optimization, less sensitive to local design changes than MFCC, and can still produce valuable designs which require only slight manual correction.

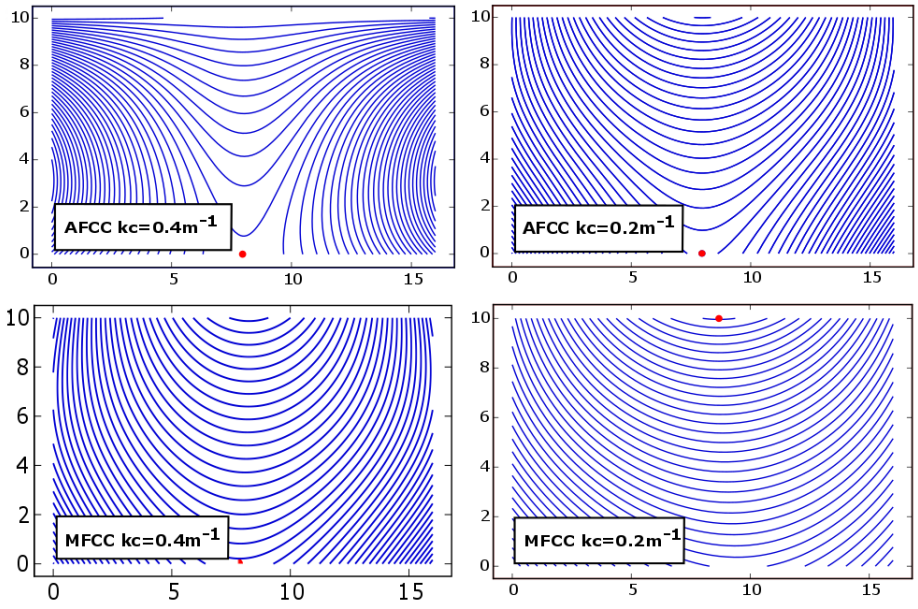

Figure 4: Results of the first test case for AFCC constraints (top row) and MFCC constraints (bottom row). Red dots indicate points of maximum curvature.

To illustrate the performance of the optimizer, the case for MFCC with a threshold of 0.4 m^{-1} is shown here exemplarily, i.e. for the result given in Fig. 4,

bottom, left. The optimization using the genetic algorithm (population size: 70, iterations: 70) was stopped after 4,900 FE evaluations, reaching sufficient convergence without constraints violation as shown in Fig. 5.

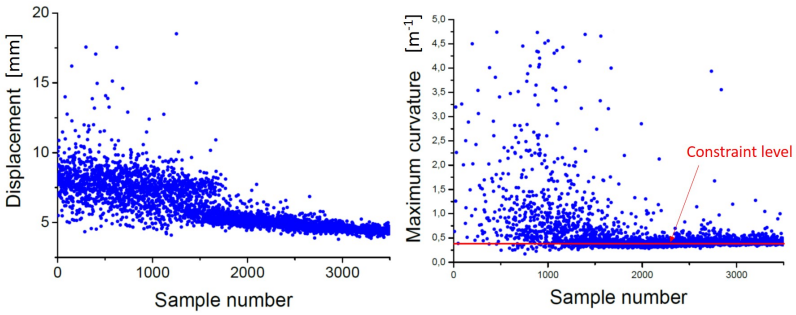

Figure 5: Exemplary optimization performance of the first test case for an MFCC constraint of 0.4 m^{-1}.

Clamped plate under uniform load: A second case, a clamped plate under uniformly distributed in-plane loading, is regarded to relate the results to fiber orientations derived by alternative approaches from the literature (here the PhD thesis of Setoodeh [15]). A fiber-steering optimization of a clamped composite plate loaded by a uniform load on the top is realized (see Fig. 6, top row). As the objective, minimization of the average displacement of the top line is considered. The control points for the surface are again equally distributed; we define here a grid of 16 (4×4) control points. Because the reference solution is derived without curvature control, our result is also given here without AFCC or MFCC values.

The results shown in Fig. 6 from the proposed method (third row) and the reference method (bottom row) do not match perfectly, which is due to the fact that different methods and therefore optimization problems have been regarded. Nevertheless, the two distributions are comparable and show similar main features. In the top and bottom element rows, both structures show horizontal fiber orientations (except in the corners). There is a rapid change in orientation along a horizontal line a little above the center line. Main differences between both solutions appear at the very right of the structure, which can be explained by the fact that the stress distribution there is very low and therefore fiber orientation is of minor importance.

To show that the proposed method can not only derive comparable results to established approaches but is also able to include smoothness considerations, i.e. curvature constraints, additional results are shown here, which cannot be compared to the reference solution obtained without any constraints. The corresponding isoline results are depicted in Fig. 7.

A closer look on the obtained displacement values (see Table 2) suggests, that less strict MFCC requirements results in a better design stiffness, meaning that these two design goals, fiber smoothness and compliance/displacement are contradictory. In this case existence of Pareto front is expected, which can be found using multi-objective optimization. This is, however, out of the scope

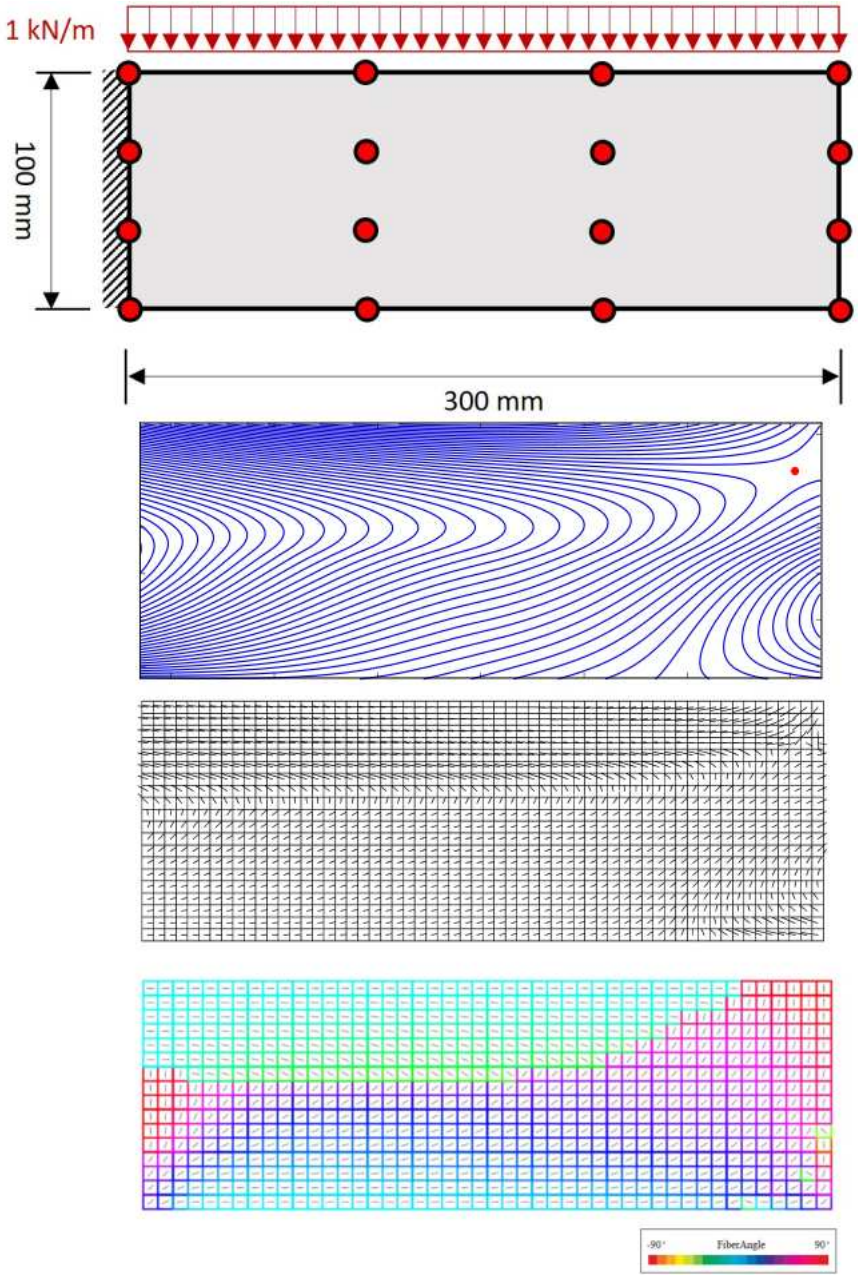

Figure 6: Optimization result of the second test case (no curvature constraint): top row: problem definition; second row: optimal isolines; third row: corresponding fiber orientations; bottom row: reference solution [15].

of the current work, which is concentrated on the validation and illustration of the proposed iso-contour method. To finalize this, a third and last example is regarded next.

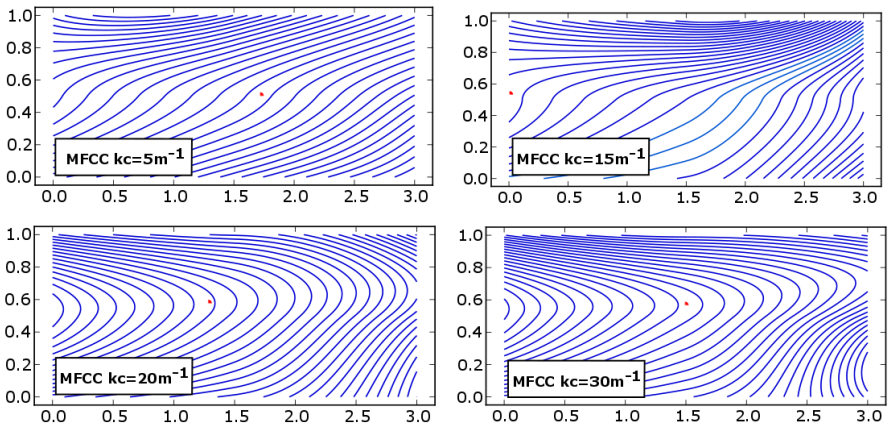

Figure 7: Optimal isolines for the second test case with different curvature constraints k_c.

Table 2: Average top line displacements for optimal fiber placement w.r.t. 0° simple laminate solution.

	0°	Fiber-steered laminates			
$k_c[m^{-1}]$	-	∞	30	20	15	5
δ_{avg}	1.0	1.79	1.78	1.74	1.41	1.23

Uni-axial buckling of a cylindrical plate with a hole: The third test case considers a cylindrically curved composite structure with a circular hole (see Fig. 8) in order to maximize the critical buckling load. This case is motivated by geometry and loading conditions from a simplified representation of a fuselage section design with a window; first results were published without details in [36, 34] and the full details are given here. Via this example, the application of the proposed iso-contour method to multiple-ply fiber steering problems is discussed. Besides the challenge how to handle multiple plies and their curvature constraints simultaneously, an additional complexity is added here by the non-linearity of the buckling problem. The plate is simply supported at the straight edges and subjected to uni-axial pressure at the curved edges, as shown in Fig. 8. The dimensions of the plate are in-plane $0.5\,\mathrm{m} \times 0.5\,\mathrm{m}$ with a total laminate thickness of 1 mm. The radius of the curvature is 0.75 m, and the radius of the centered hole is 0.12 m. Two different laminate designs are considered, each having four layers: $[\pm\alpha]_s$ and $[\alpha, \alpha + 90°]_s$, where α is the local fiber angle in the design layer. In order to test how the number of control points influences the optimal fiber paths, three different grids with 3×3, 4×4 and 5×5 control points are defined over the 2D plate-projection domain. Thus, the number of design variables for this test case is equal to 9, 16 or 25. Several optimizations with different maximum curvature constraint bounds are performed, starting with an unconstrained case, followed by MFCC of 5, 10, and 20 m^{-1}.

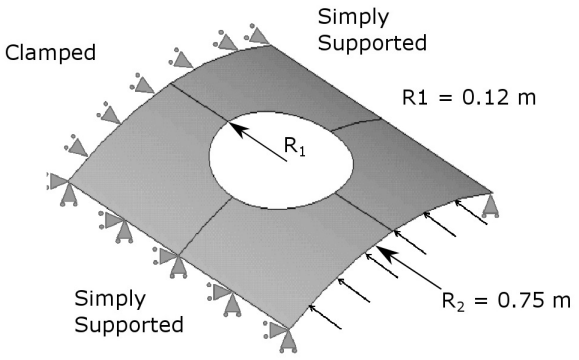

Figure 8: Clamped curved composite structure with 4 plies $[\pm\alpha]_s$ and $[\alpha, \alpha + 90°]_s$.

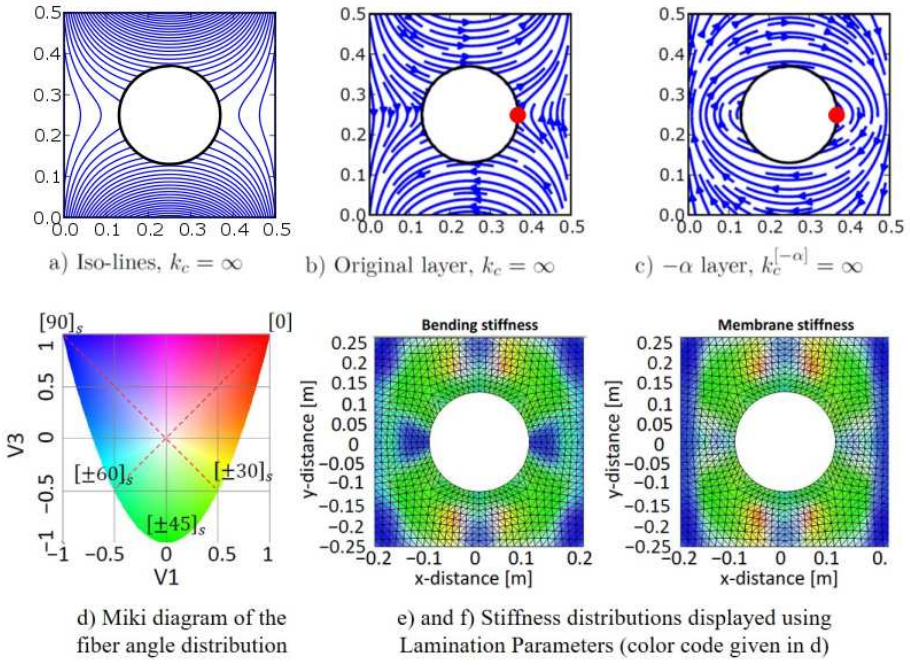

Figure 9: Top row: isolines and fiber orientations for the curved structure with hole and 4 plies $[\pm\alpha]_s$ without considering curvature constraints; bottom row: results from [42] using lamination parameters V_1, V_3 showing comparable fiber orientations.

The optimal fiber distributions for the unconstrained problem obtained by the proposed Iso-Contour Method for $[\pm\alpha]_s$ layers and 3×3 control points are shown in the top row of Fig. 9, with the maximum curvature location indicated by a red point for each layer. This can be compared to results from literature;

Table 3: Final values of the objective for $[\pm\alpha]_s$ design and different k_c values. Values of critical buckling loads are normalized with respect to the critical load for $[\pm 45°]_s$ laminate.

	$[\pm 45°]_s$	Fiber-steered laminates			
$k_c[m^{-1}]$	-	∞	20	10	5
P_{cr}	1.0	1.89	1.83	1.766	1.502

e.g. Hesse [42] used Lamination parameters (LPs) V_1, V_3 to derive the optimal stiffness distributions and orientations for bending and membrane stiffnesses (bottom row of Fig. 9). The colors represent the angles according to the Miki diagram also given in the same figure. Comparing the top and the bottom rows, it can be seen that the obtained results via the ICM are in good agreement with those obtained using LPs; the fibers are nearly straight (i.e. $[90°]_s$) near the straight edges (blue areas in Fig. 9, bottom row). Near the hole in the center, the fibers have a $[\pm 45°]_s$ orientation indicated by the green color in Fig. 9, bottom row). This corresponds roughly to the fiber orientations shown in the top row obtained by the proposed method. Note, that these results are obtained for the unconstrained case where no curvature constraint is considered.

Optimized designs for the constrained cases (MFCC with 5, 10, 20 m^{-1}) for the same type of composite, i.e. the $[\pm\alpha]_s$ laminate design and the same number of 3×3 control points are shown in Fig. 10 with corresponding critical buckling forces given in Table 3. A global design change can be observed when the MFCC limit is increased from 5 to 10 m^{-1}; for higher MFCC values, circular paths are obtained around the hole.

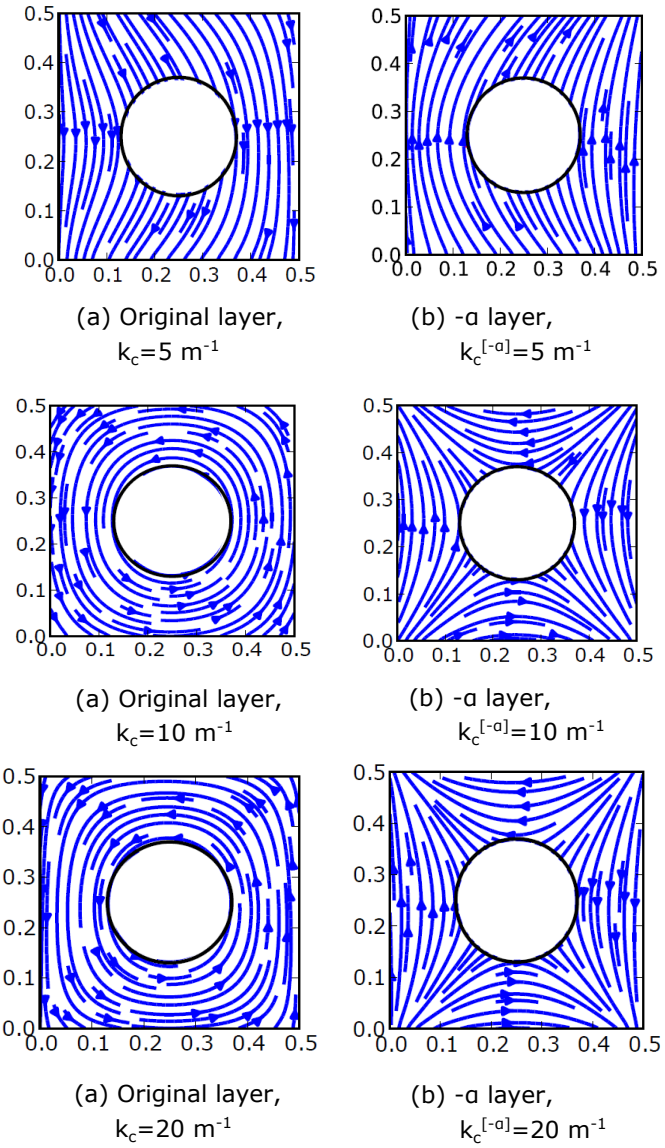

Figure 10: Fiber orientations for the curved structure with hole and 4 plies $[\pm\alpha]_s$ with consideration of the MFCC curvature constraint for different critical curvatures k_c.

For the next study, the laminate design is changed to $[\alpha, \alpha + 90°]_s$. The results obtained for the constrained ($k_c = 5\,\mathrm{m}^{-1}$) for different number of control points are shown in Fig. 11 and are summarized in Table 4. Concerning the critical buckling load, $[\alpha, \alpha + 90°]_s$ laminate design provides a better buckling resistance compared to the $[\pm\alpha]_s$ stacking with 3×3 grid. Also the variation of the number of control points has a clear influence on optimal results; as expected, more control points provide higher fiber path flexibility to improve the objective while satisfying complicated maximum curvature constraints.

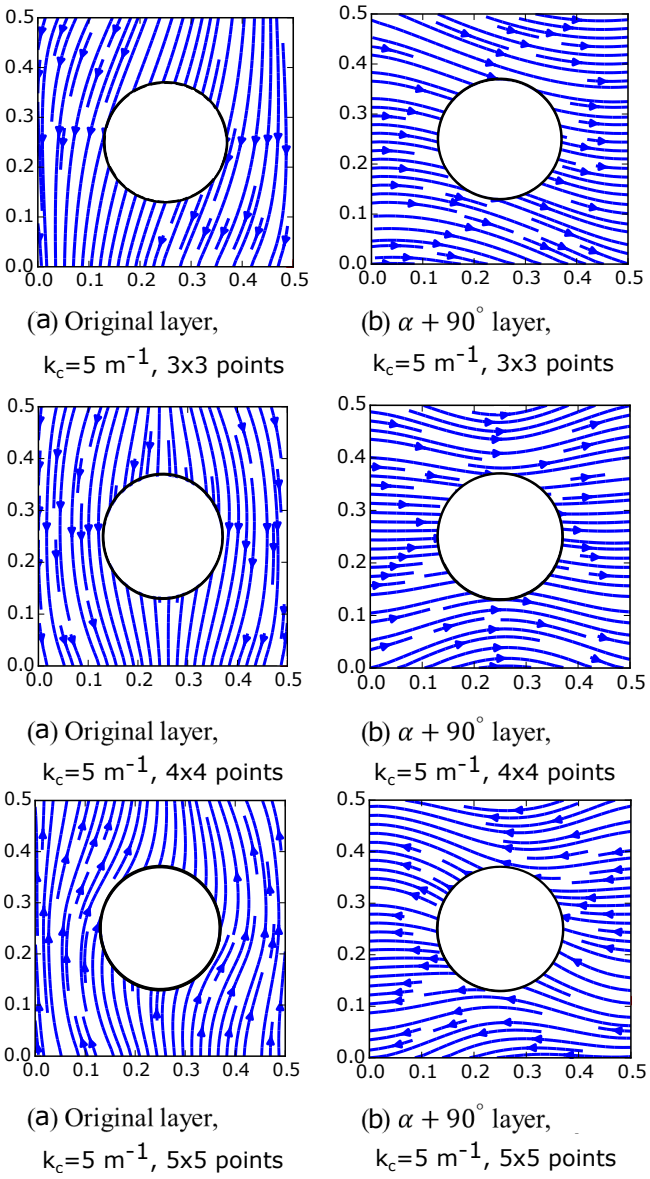

Figure 11: Fiber orientations for the curved structure with hole and 4 plies $[\alpha, \alpha + 90°]_s$ with consideration of the MFCC curvature constraint for $k_c = 5\,\mathrm{m}^{-1}$.

6 Wingbox rib optimization using the Iso-Contour Method

This section shows an application of the proposed method to the realistic engineering problem, the optimization of a single rib of a wingbox of an aircraft.

Table 4: Final values of the objective for $[\alpha, \alpha + 90°]_s$ design with $k_c = 5\,\mathrm{m}^{-1}$ for different number of control points. Values of critical buckling loads are normalized with respect to the critical load for a $[\pm 45°]_s$ laminate.

	$[\pm 45°]_s$	Fiber-steered laminates		
$k_c[m^{-1}]$	-	5×5	4×4	3×3
P_{cr}	1.0	1.839	1.726	1.641

For this, the rib is treated as a sub-structure of the total wing structure. The corresponding load definition originates from a hierarchical wingbox optimization approach developed in [37]. This means, a complete optimization of the wing is not presented here, but a representative rib optimization is discussed to show the potential of the proposed fiber-steering optimization.

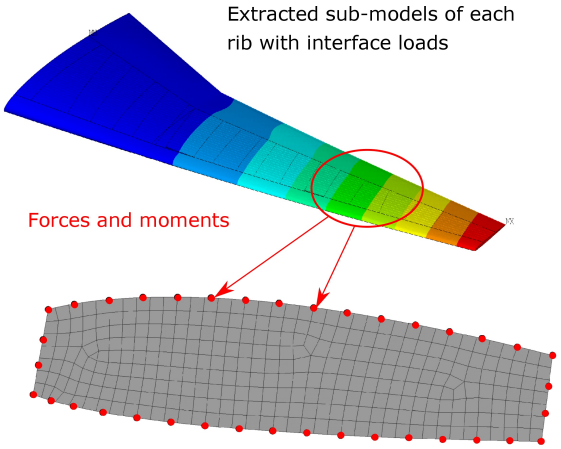

Figure 12: Top: full wing model with a result from a static bending analysis concerning static aerodynamic loads and weight from [37]. Bottom: extracted exemplary rib with interface nodes where the interface conditions (forces / moments) are defined.

For current study it is assumed, that the wing design is already optimized on the global level (e.g. shape of the wing and shapes of the airfoil cross-sections, stringers and other global reinforcements). Then, the rib can be optimized in a decoupled manner on a lower level of the overall hierarchical scheme. For this, the rib is cut out from the full wingbox model after the complete wing is computed/optimized w.r.t. appropriate load cases. Here, wing loading at cruise conditions is considered. The interface loads, in this case static forces and moments at the nodes of the outer circumference of the rib as shown in Fig. 12, are automatically extracted from the full model and applied to the rib sub-model using multi-point constraints (MPCs). These are special equations, connecting multiple degrees of freedom (DoFs) in the FE model, used here

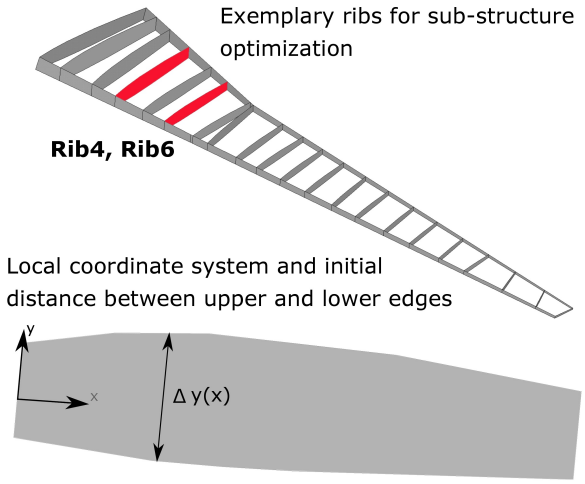

Figure 13: Top: full wing structure with two exemplary ribs for rib optimization from [37]. Bottom: local coordinate system with definition of the initial dimension in local y-direction.

to distribute the loads from the locations of the nodes of the full model onto much finer interface nodes of the sub-model, see Fig. 12. Sure, this decoupled approach does not consider full interaction between wing and rib structures and a complete iterative loop is required. Nevertheless, this is not the purpose of this paper; here, we want to demonstrate the fiber-steering optimization with the new curvature constraint handling.

The rib optimization problem is now defined as follows: the total stiffness of the rib should be maximized, to ensure that the outer surface of the wing does not deform so much and the aerodynamically optimized performance is maintained. Hence, the proposed objective function is defined as the average change of the rib height profile under the pre-defined nodal loads, which reflects the changes of the aerodynamic profile of the wing in the defined flight situation. This corresponds to using the rib local coordinate system and computing the relative deformation in local y-direction between lower and upper rib sides (see Fig. 13, bottom).

Optimization results are presented here for two exemplary ribs (Rib 4 and Rib 6, shown in red in Fig. 13, top). Several optimization studies are performed with various composite designs, including single-layer and symmetric $[\pm\alpha]_s$ four-layer configurations. A number of optimizations with different maximum curvature constraint bounds are performed including an unconstrained case, followed by MFCC with $k_c = 10, 20\,\mathrm{m}^{-1}$, depending on the actual rib dimensions. In total 15 control points (3×5 grid) are distributed regularly over the rib, placing more points along the local x-direction.

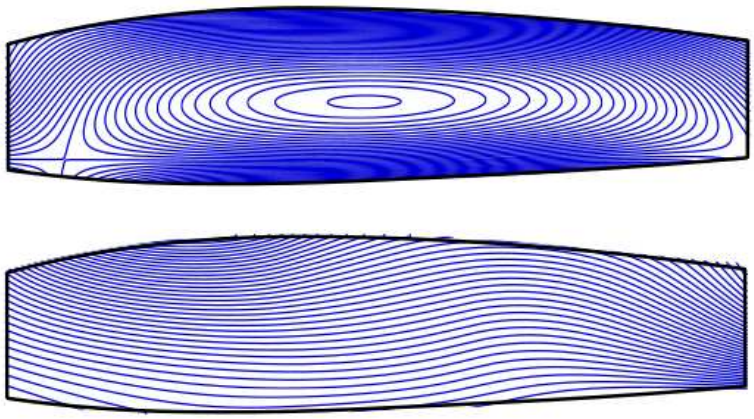

Figure 14: Isolines for the unconstrained case (top) and for the constrained case (bottom) with an MFCC with $k_c = 10\,\mathrm{m}^{-1}$; (both results are derived for the single layer composite).

The results for the single layer case are shown in Fig. 14 for the unconstrained (top) and constrained (bottom) optimization cases for Rib 6. The influence of the curvature constraint is relatively high for the case regarded here. The introduction of the MFCC constraint significantly complicates the task. Overall, 15,000 evaluations are realized for both cases; the unconstrained case reaches reasonable designs relatively early while the constrained needs around 5,000 samples to get into the feasible area since a lot of good designs with violated constraint are rejected at the beginning. Finally, results for the composite rib with 4 layers ($[\pm\alpha]_s$ case) are shown for the constrained and unconstrained cases, see Fig. 15, 16.

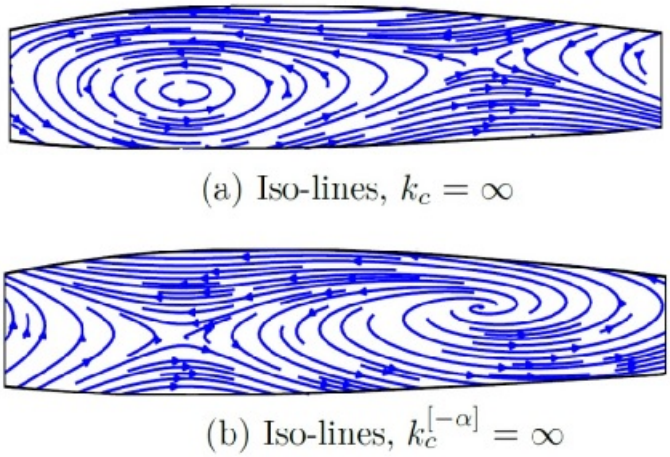

(a) Iso-lines, $k_c = \infty$

(b) Iso-lines, $k_c^{[-\alpha]} = \infty$

Figure 15: Fiber orientations for the unconstrained case; (results are derived for the 4-layer composite with $[\pm\alpha]_s$).

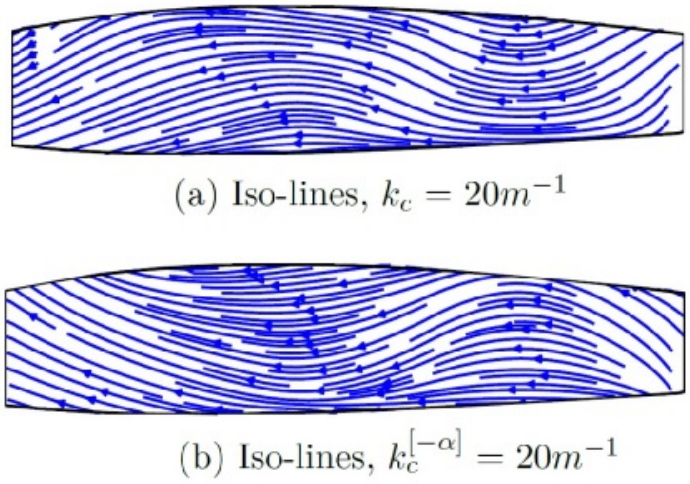

(a) Iso-lines, $k_c = 20m^{-1}$

(b) Iso-lines, $k_c^{[-\alpha]} = 20m^{-1}$

Figure 16: Fiber orientations for the constrained case with an MFCC with $k_c = 20\,\mathrm{m}^{-1}$; (results are derived for the 4-layer composite with $[\pm\alpha]_s$).

7 Conclusions

In this paper, a novel method for parametrization and optimization of fiber-steered composite designs is presented based on iso-contours of an artificial smooth surface. The corresponding isolines of this artificial surface represent fiber paths in fiber-steered composite laminate plies. The method is able to accurately handle maximum fiber curvature constraint (MFCC) for mono- or multi-layered fiber-steered composites; this was shown exemplarily for composites with $[\pm\alpha]_s$ and $[\alpha, \alpha + 90°]_s$ 4-layer structures where the maximum curvature can differ significantly for different layers. The method was validated against available test cases and its capabilities were illustrated using several examples, which confirmed the parametrization flexibility and accurate constraints handling. Depending on the manufacturing constraints, it was shown how the method is able to switch between different optimal fiber placement patterns, thanks to the non-local optimization. Finally, the iso-contour fiber paths optimization is applied to improve designs for the composite wing box ribs.

The combination of a low-dimensional flexible parame-trization, a global derivative-free optimization approach and an accurate handling of maximum curvature constraints for multilayered laminates are the features, which make the proposed approach attractive for many applications. In future research, limitations and benefits of the proposed method should be analyzed especially by a comparison with the existing approaches. In addition, the method can be extended for periodic cases, such as cylindrical shells, or other more complex examples. From a numerical viewpoint, the speed of optimization convergence and the overall effort may be evaluated. More advanced optimization techniques, including speed-up due to local gradient-based searches with smoothed maximum curvature constraints, may be interesting.

8 Acknowledgements

The financial support for the European project Marie Curie Actions, Research Fellowship Programme, 7th Framework Programme (FP7), 'Aerospace Multi-disciplinarity Enabling DEsign Optimisation' (AMEDEO) through EU grant reference 316394 is gratefully acknowledged, see also [43] and https://cordis.europa.eu/project/rcn/105135/factsheet/en.

References

[1] Lukaszewicz DH-J, Ward C, Potter KD (2012). The engineering aspects of automated prepreg layup: History, present and future. Composites Part B: Engineering 43(3): 997–1009.

[2] Alhajahmad A, Abdalla MM, Gürdal Z (2008). Design tailoring for pressure pillowing using tow-placed steered fibers. Journal of Aircraft 45(2): 630–640.

[3] Blom AW, Abdalla MM, Gürdal Z (2010). Optimization of course locations in fiber-placed panels for general fiber angle distributions. Composites Science and Technology 70(4): 564–570.

[4] Abdalla MM, Setoodeh S, Gürdal Z (2007). Design of variable stiffness composite panels for maximum fundamental frequency using lamination parameters. Composite Structures 81(2): 283–291.

[5] van Campen JMJF, Kassapoglou C, Gürdal Z (2012). Generating realistic laminate fiber angle distributions for optimal variable stiffness laminates. Composites Part B: Engineering 43(2): 354–360.

[6] Ghiasi H, Fayazbakhsh K, Pasini D, Lessard L (2010). Optimum stacking sequence design of composite materials Part II: Variable stiffness design. Composite Structures 93(1): 1–13.

[7] IJsselmuiden ST, Abdalla MM, Gürdal Z (2010). Optimization of variable-stiffness panels for maximum buckling load using lamination parameters. AIAA Journal 48(1): 134–143.

[8] Marouene A, Boukhili R, Chen j, Yousefpour A (2016). Buckling behavior of variable-stiffness composite laminates manufactured by the tow-drop method. Composites Structures 139: 243–253.

[9] Setoodeh S, Abdalla MM, IJsselmuiden ST, Gürdal Z (2009). Design of variable-stiffness composite panels formaximum buckling load. Composite Structures 87(1): 109–11.

[10] Hesse S, Lukaszewicz D, Duddeck F (2015). A method to reduce design complexity of automotive composite structures with respect to crashworthiness. Composite Structures 129: 236–249.

[11] Biggers SB, Srinivasan S (1993). Compression buckling response of tailored rectangular composite plates. AIAA Journal 31(3): 590—596.

[12] Biggers SB, Pageau SS (1994). Shear buckling response of tailored composite plates. AIAA Journal 32(5): 1100—1103.

[13] Hyer MW, Charette RF (1991). Use of curvilinear fiber format in composite structure design. AIAA Journal 29(6): 1011-–1015.

[14] Setoodeh S, Gürdal Z (2003). Design of composite layers with curvilinear fiber paths using cellular automata. 44th AIAA/ASME/ASCE/AHS/ASC Structures, Structural Dynamics, and Materials Conference, Norfolk, VA, USA.

[15] Setoodeh S (2005). Optimal design of variable-stiffness fiber-reinforced composites using cellular automata. PhD thesis. Technische Universiteit Delft, Delft, The Netherlands.

[16] Gürdal Z, Olmedo RA (1992). Composite laminates with spatially varying fiber orientations: variable stiffness panel concept. 33rd AIAA/ASME/ASCE/AHS/ASC Structures, Structural Dynamics, and Materials Conference. Dallas,TX, USA.

[17] Gürdal Z, Olmedo RA (1993). In-plane response of laminates with spatially varying fiber orientations - Variable stiffness concept. AIAA Journal 31(4): 751–758.

[18] Alhajahmad A, Abdalla MM, Gürdal Z (2010). Optimal design of tow-placed fuselage panels for maximum strength with buckling considerations. Journal of Aircraft 47(3): 775-–782.

[19] Stanford B, Wieseman CD, Jutte C (2015). Aeroelastic tailoring of transport wings including transonic flutter constraints. 56th AIAA/ASCE/AHS/ASC Structures, Structural Dynamics, and Materials Conference, AIAA SciTech Forum, (AIAA 2015-1127).

[20] Huang J, Haftka RT (2005). Optimization of fiber orientations near a hole for increased load-carrying capacity of composite laminates. Structural and Multidisciplinary Optimization 30(5): 335–341.

[21] Brooks TR, Hwang JT, Kennedy GJ, Martins JRRA (2015). High-fidelity structural optimization of a tow-steered composite wing. 11th World Congress on Structural and Multidisciplinary Optimization. Sydney, Australia.

[22] Honda S, Igarashi T, Narita Y (2013). Multi-objective optimization of curvilinear fiber shapes for laminated composite plates by using NSGA-II. Composites Part B: Engineering 45(1): 1071–1078.

[23] IJsselmuiden S (2011). Optimal design of variable stiffness composite structures using lamination parameters. PhD thesis, Technische Universiteit Delft, Delft, The Netherlands.

[24] Fukunaga H, Vanderplaats G (1991). Stiffness optimization of orthotropic laminated composites using lamination parameters. AIAA Journal 29(4): 641–646.

[25] Miki M, Sugiyama Y (1993). Optimum design of laminated composite plates using lamination parameters. AIAA Journal 31(5):921–922.

[26] Tsai SW, Halpin JC, Pagano NJ (1968). Composite materials workshop. Technomic Publ., Stamford, CT, USA.

[27] Tsai SW, Hahn T (1980). Introduction to composite materials. Technomic Publ., Westport, CT, USA.

[28] Grenestedt JL, Gudmundson P (1993). Lay-up optimisation of composite material structures. Proc. IUTAM Symp. on Optimal Design with Advanced Materials, pp. 311–336. Elsevier, Amsterdam, The Netherlands.

[29] van Campen JMJF, Kassapoglou C, Gürdal Z (2011). Design of fiber-steered variable-stiffness laminates based on a given lamination parameters distribution. 52nd AIAA/ASME/ASCE/AHS/ASC Structures, Structural Dynamics, and Materials Conference, Denver, CO, USA.

[30] van Campen JMJF (2011). Optimum lay-up design of variable stiffness composite structures. PhD thesis, Technische Universiteit Delft, Delft, The Netherlands.

[31] Setoodeh S, Blom A, Abdalla MM, Gürdal Z (2006). Generating curvilinear fiber paths from lamination parameters distribution. 47th AIAA/ASME/ASCE/AHS/ASC Structures, Structural Dynamics, and Materials Conference, Newport, RI, USA.

[32] Klees JC, Ijsselmuiden ST, Abdalla MM, Gürdal Z (2009). Fibre angle reconstruction for variable-stiffness panels including curvature constraints. Europ. Conf. on Spacecraft Structures, Materials & Mechanical Testing (ECSSMMT), Toulouse, France.

[33] Nagendra S, Kodiyalam S, Davis J, Parthasarathy V (1995). Optimization of tow fiber paths for composite design. 36th Structures, Structural Dynamics, and Materials and Co-located Conferences. New Orleans, LA, USA.

[34] Hesse S, Arsenyeva A, Lukaszewicz D, Duddeck F (2015). A parameterized surface method to determine optimal variable stiffness layup design by global search. 20th Int. Conf. on Composite Materials (ICCM), Copenhagen, Denmark.

[35] Arsenyeva A, Duddeck F (2014). Iso-contour method for optimization of steered-fiber composites. 10th ASMO UK / ISSMO Conf. on Engrg Design Optimization, Delft, The Netherlands.

[36] Arsenyeva A, Duddeck F (2016). Optimization of fiber-steered composites by using the Iso-contour Method with maximum curvature constraint. 17th Europ. Conf. for Composite Materials (ECCM17), Munich, Germany.

[37] Arsenyeva, A (2020). Level-dependent Optimization Methods for Metal and Composite Wingbox Structures. PhD thesis, Technical University of Munich. Schriftenreihe des Fachgebiets für Computational Mechanics, Shaker.

[38] Forrester AIJ, Sóbester A, Keane AJ. Engineering Design via Surrogate Modelling - A Practical Guide. Wiley, 2008.

[39] Theisel H (1995). Vector Field Curvature and Applications. PhD thesis, University of Rostock, Germany.

[40] Dakota Users Guide, Version 6.17, https://snl-dakota.github.io/docs/6.17.0/users/, date of retrieval 11 June, 2023.

[41] Eldred MS, Adams BM, Dalbey KR, Swiler LP (2011). DAKOTA, a multilevel parallel object-oriented framework for design optimization, parameter estimation, uncertainty quantification, and sensitivity analysis. Version 5.2 Reference Manual. Sandia National Laboratories Albuquerque. NM, USA.

[42] Hesse SH. Multi-objective design optimization of steered composite structures. MSc thesis, Technische Universiteit Delft, Delft, The Netherlands.

[43] Aissa M, Chahine C, Arsenyeva A, Baumgärtner D, Bletzinger K-U, Duddeck F, Basdogan I, Serhat G, Bettebghor D, Bordogna M, Carrier G, Lancelot P, Viti A, de Breuker R, Jovanov K, Caloni S, Clayton G, Shahpar S, Duckitt S, Weustink T, Hewson R, Ollar J, Surry T, Pohl J, Thompson H, Schlaps R, Verstraete T, Toropov V (2016). Multidisciplinary Design Optimisation Research Contributions from the AMEDEO Marie Curie Initial Training Network. Proc. 11th ASMO UK / ISSMO Conf. Engineering Design Optimization, Product and Process Improvement / NOED2016, Technische Universität München, Munich, Germany.